

The Antiferromagnetic and Phonon-mediated Model of the NaFeAs, LiFeAs and FeSe Superconductors

Wong Chi Ho^{1,2,*}, Rolf Lortz^{1,*}

¹Department of Physics, Hong Kong University of Science and Technology, Hong Kong

²Institute of Physics and Technology, Ural Federal University, Yekaterinburg, Russia

Email address:

ch.kh.vong@urfu.ru (Wong Chi Ho), lortz@ust.hk (Rolf Lortz)

*Corresponding author

Abstract: Recently it has been suggested that the role of electron-phonon coupling in the mechanism of iron-based superconductors may have been underestimated and that the antiferromagnetism and the induced xy potential may even have a dramatic amplification effect on electron-phonon coupling. To substantiate the recently announced xy potential in the literature, we create a two-channel model to separately superimpose the dynamics of the electron in the upper and lower tetrahedral plane. The results of our two-channel model support the literature data. While the scientists are still searching for a universal DFT functional that can describe the pairing mechanism of all iron-based superconductors, we are designing an empirical combination of DFT functional to calculate the electron-phonon coupling and antiferromagnetism of LiFeAs, NaFeAs and FeSe. We use ARPES data to revise the electron-phonon scattering matrix in superconducting state to ensure that all electrons involved in iron-based superconductivity are included in the ab-initio calculation. We present an ab-initio theoretical approach that takes into account this amplifying effect of antiferromagnetism and the correction of the electron-phonon scattering matrix together with the abnormal soft out-of-plane lattice vibration of the layered structure, which allows us to calculate theoretical T_c values of LiFeAs, NaFeAs and FeSe as a function of pressure that correspond reasonably well to the experimental values.

Keywords: Iron-based Superconductivity, Ab-initio Method, T_c Calculation

1. Introduction

The pairing mechanism of the unconventional high-temperature superconductors (HTSC) remains one of the greatest unsolved mysteries of physics. All unconventional superconductors, including cuprates [1, 2] and iron-based HTSC [3, 4], but also heavy fermions [5] and organic superconductors [6], have in common that the superconducting phase occurs near a magnetic phase. Furthermore, their phase diagrams typically show at least one other form of electronic order, e.g. charge or orbital order [7, 8], a pseudogap phase [2], stripe order [2] or nematic order [9]. The proximity of the magnetic phases naturally suggests the involvement of magnetism [10]. In most theoretical approaches, spin fluctuations play a leading role [11, 12]. Alternative approaches consider e.g. excitonic superconductivity [13, 14], long-wavelength plasmonic charge fluctuations or orbital fluctuations [15-17].

It is generally assumed that the Cooper pairing in these superconductors cannot be described within a standard phonon-mediated scenario. However, this assumption is based only on the consideration of electron-phonon coupling on the Fermi surface only. The T_c calculation based on the McMillan T_c formula typically uses an approximation valid for classical low- T_c superconductors, where the superconducting electron concentration is only considered at the Fermi level. This approximation is no longer valid for high-temperature superconductors such as the iron-based superconductors, since high-energy phonons are excited at elevated temperatures, so that electron-phonon scattering influences the electron over a larger energy range around the Fermi energy. In the high temperature limit, where phonons are excited to the Debye energy, this energy interval becomes. Experimental ARPES data actually show that in iron-based superconductors electrons down to ~ 0.03 - 0.3 eV below the Fermi energy are influenced by the onset of superconductivity [28-30]. In order to perform a meaningful and convincing study of whether the electron-phonon coupling is related to the formation of Cooper pairs in iron-based superconductors or not, we decide to consider the true superconducting electron concentration in order to recalculate the electron-phonon coupling constant under antiferromagnetic background. Several studies offered an alternative scenario for iron-based superconductors, suggesting that the role of electron-phonon coupling had previously been underestimated against the antiferromagnetic (AF) background [18-20]. An explicit DFT calculation by B. Li et al [19] showed that the phonon softening of AFeAs (A: Li or Na) under AF background allows an increase of the electron-phonon coupling by a factor of ~ 2 . While any orthogonal change of the phonon vector can be considered a phonon softening phenomenon, the lattice dynamics studied by S. Deng et al [20] confirmed that out-of-plane lattice vibration amplifies electron-phonon scattering based on their first-principle linear response calculation. While the tetrahedral atom is better suited to attract electrons in terms of electronegativity, the vertical displacement of the lattice Fe transfers the charge of the electron to the tetrahedral regions to generate an additional xy

potential [18]. S. Coh et al [18] calibrated the GGA+A functional, which made it possible to bring the simulation results much closer to the experiments [42]. The calibrated ab-initio method explicitly demonstrate the occurrence of the induced xy potential from the out-of-plane lattice dynamics in the AF background that increase the electron-phonon scattering matrix by this factor of ~ 2 (abbreviated as ratio R_{ph}). More importantly, they provide an analytical model [18] to explain why the electron-phonon scattering computed by the ab-initio method is always increased by a ratio of ~ 2 under the effect of the spin density wave (abbreviated as ratio R_{SDW}).

In this article, we revise the superconducting electron concentration and use an ab-initio approach to explicitly calculate the T_c values of LiFeAs, NaFeAs and FeSe at ambient pressure by taking into account the R_{ph} and R_{SDW} factors in the electron-phonon scattering mechanism to test whether the combination of the abnormal out-of-plane lattice vibration together with the AF effect could actually provide the experimentally observed high T_c values. We also model the pressure dependence of T_c by monitoring the AF exchange Hamiltonian as a function of pressure. Our T_c values are qualitatively consistent with the experimental values, suggesting to further explore the possibility of antiferromagnetically-assisted electron-phonon coupling as a possible superconducting mechanism in iron based superconductors.

2. Computational Methods

As starting point, the electronic band diagram and density of states (DOS) of all compounds investigated in this article are computed in the program package WIEN2k. The phonon data are calculated in finite displacement mode. The experimental lattice parameters are used [25, 26]. The spin-unrestricted GGA-PBE functional [21-23] is used (unless otherwise specified). In this article only Fe and As atoms are imported for the 111-type compounds. Due to length restrictions we show the raw data of ab-initio calculation in the supplementary materials. In this article we focus on the effect of magnetically enhanced electron-phonon coupling.

Instead of calibrating 'A' in the GGA+A functional, which entails an enormous computational cost and time-consuming experimental effort [18, 41, 42], we propose a two-channel model to more easily model the induced xy potential, where the upper tetrahedral plane is called channel 1 and the lower tetrahedral plane is called channel 2, respectively. We apply the superposition principle to separately calculate the induced xy potentials induced by channel 1 and 2. Our two-channel model has fulfilled an assumption that the probability of finding an Fe atom moving in the $+z$ and $-z$ directions is equal, but that their vibrational amplitudes never cancel each other out. This assumption is justified by Coh *et al* whose explicit calculation confirms that the iron-based system consists of an out-of-phase vertical displacement of iron atoms, with first adjacent iron

atoms moving in opposite directions [18]. We define $R_{ph} = \frac{0.5(DOS_1^{XY} + DOS_2^{XY})}{DOS_{12}^{XY}}$ where DOS_c^{XY} is the average electronic density of states within the ARPES range. The index c refers to the channel index.

Define $F(\omega)$ is the phonon density of state as a function of frequency ω and the integral $\int d^2 p_F$ is taken over the Fermi surface with the Fermi velocity v_F . The Eliashberg function is written as [27]

$$\alpha^2 F(\omega) = \int \frac{d^2 p_F}{v_F} \int \frac{d^2 p'_F}{(2\pi\hbar)^3 v_F} \sum_v g_{pp'v}^2 \delta(\omega - \omega_{p-p'v}) / \int \frac{d^2 p_F}{v_F}$$

The electron-phonon matrix elements is given by $g_{pp'v} = \sqrt{\frac{\hbar}{C\omega_{p-p'v}}} g_v(p, p')$ where

$\int \psi_p^* u_i \cdot \nabla V_{XY} \psi_{p'} dr$ is abbreviated as $g_v(p, p')$ and C is the material constant related to lattice [27]. The u_i and V_{XY} represent the displacement of ion relative to its equilibrium position and the ionic potential. The $\psi_p^* \psi_p$ is the electronic probability density in the non-magnetic state. The resultant ionic interaction V_{ion}^{XY} on the XY plane due to the abnormal phonon is calculated by multiplying the ionic potential by R_{ph} , i.e. $V_{ion}^{XY} = V_{XY} \cdot R_{ph}$. Moreover, the antiferromagnetic interaction along the XY plane amends the electronic probability density which fulfills $\phi_p^* \phi_p \sim \psi_p^* R_{SDW} \psi_p$ where the spin density wave factor R_{SDW} is directly obtained from the ab-initio calculation. Rearranging the mathematical terms yields the electron-phonon matrix element. as

$$g_{pp'v} = \sqrt{\frac{\hbar}{C\omega_{p-p'v}}} \int u_i \cdot \nabla (V_{XY} R_{ph}) \psi_p^* R_{SDW} \psi_p dr = \sqrt{\frac{\hbar}{C\omega_{p-p'v}}} \int \phi_p^* u_i \cdot \nabla V_{ion}^{XY} \phi_p dr$$

To derive a superconducting transition temperature from the computed parameters, we use the McMillan T_c formula [27]. Due to the high transition temperatures, the electron-phonon scattering matrix takes into account the full electronic DOS in range of $E_F - E_{Debye}$ to E_F and not only the value at Fermi level. Here we consider the fact that E_{Debye} represents the upper limit of the phonon energies that can be transferred to electrons, and at the high transition temperatures of Fe-based superconductors, contributions from high energy phonons become important in the electron-phonon scattering mechanism, as opposed to classical low- T_c superconductors. Although this approach is a simple consequence of the conservation of energy, it is supported by experiments: A shift of the spectral weight between the normal and the superconducting state is clearly visible in the photoemission spectra below the superconducting energy gap of various iron-based compounds in an energy range of ~30 - 60 meV below the Fermi energy [28-30]. This energy range is approximately in the order of the Debye energy.

In BCS superconductors, the electrons on the Fermi surface condense into the Bose-Einstein superconducting state where the total number of electrons on the Fermi surface equals to the total number of electrons on the superconducting state. Hence, the theoretical T_c of BCS superconductors remain the same if we substitute either the electronic DOS on the Fermi level or the electronic DOS of the condensed Bose-Einstein state. However, the situation is different in iron-based superconductivity where the electrons located between $E_F - E_{Debye}$ and E_F transfer energy to the electrons in the Bose-Einstein superconducting states. When this happens, we have to revise the resultant electron-phonon scattering matrix in the condensed Bose-Einstein state. Bose-Einstein statistic favors more electrons occupying in the superconducting state. The electrons within ARPES range increases the electronic DOS in the condensed Bose-Einstein state indirectly. Those electrons within the ARPES range cannot be excited to the Fermi surface due to electrostatic repulsion. However, those electrons have another route to follow the Bose-Einstein distribution which can be argued as a reason why those electrons disappear below the Fermi level.

The computation of band structure produces discrete (E,k) points where E and k are the energy and the wavevector of electron.

The ratio of the electron-phonon scattering matrix is $R_g = \frac{\sum_{-\infty}^{E_F} g(E) \delta_A(E) / \sum_{-\infty}^{E_F} \delta_{counter}(E)}{\sum_{-\infty}^{E_F} g(E) \delta_B(E) / \sum_{-\infty}^{E_F} \delta_{counter}(E)}$. The $\delta_A(E)$ is 1 if

$$(E_F - E_D) \leq E \leq E_F. \text{ Similarly, the } \delta_B(E) = 1 \text{ if } E = E_F. \text{ Otherwise } \delta_A(E) = \delta_B(E) = 0. \sum_{-\infty}^{E_F} \delta_{counter}(E) \text{ gives}$$

the total number of (E,k) points in the range $-\infty \leq E \leq E_F$. $\sum_{-\infty}^{E_F} \delta_A(E) / \sum_{-\infty}^{E_F} \delta_{counter}(E)$ or $\sum_{-\infty}^{E_F} \delta_B(E) / \sum_{-\infty}^{E_F} \delta_{counter}(E)$ is

the percentage of electrons contributed to the R_g factor. To make a fair comparison, the interval of k space in the numerator and denominator of R_g are essentially the same. The R_g factor controls the proportion of electrons scattered below the Fermi level. We show an example of R_g calculation in appendix.

Due to the fact that the superconducting transition temperatures of these three superconductors are ~10K, we calculate the mean occupation number $f(E)$ in the Fermi-Dirac statistic at 10K, where $f(E_F)$ and $f(E_F - E_{Debye})$ are 0.5 and 0.5005, respectively. If $DOS(E_F) / DOS(E_F - E_{Debye}) \sim 1$, $f(E_F) / f(E_F - E_{Debye}) \sim 1$ and $E_F \gg E_{Debye}$, the tiny offset in the mean occupation number may allow the Eliashberg function to approximately obey the following form.

$$\alpha_{PS}^2 F(\omega) \sim \left\langle \sum_{V_F - V_{Debye}}^{V_F} \int \frac{d^2 p_E}{v_E} \right\rangle \left\langle \sum_{V_F - V_{Debye}}^{V_F} \int \frac{d^2 p_E'}{(2\pi\hbar)^3 v_E'} \right\rangle \sum_v \delta(\omega - \omega_{p-p'v}) \left| \sqrt{\frac{\hbar}{C\omega_{p-p'v}}} \int u_i \cdot \nabla (V_{XY} R_{ph}) \psi_p^* R_{SDW} R_g \psi_p dr \right|^2 / \left\langle \sum_{V_F - V_{Debye}}^{V_F} \int \frac{d^2 p_E}{v_E} \right\rangle$$

where $v_E \in (v_F - v_{Debye}, v_F)$ and the velocity v_{Debye} is converted from the Debye energy. $\sum_{V_F - V_{Debye}}^{V_F} \int \frac{d^2 p_E}{v_E}$ is the sum of the

surface integral $\int \frac{d^2 p_E}{v_E}$ at different electron energies within the ARPES range. The form of the antiferromagnetically amplified electron-phonon coupling is expressed as $\lambda_{PS}^{Coh} \sim 2 \int \alpha_{PS}^2 \frac{F(\omega)}{\omega} d\omega$ where $\alpha_{PS}^2 \sim \alpha_{E_F}^2 R_{ph}^2 R_{SDW}^2 R_g^2$. The α_{E_F} is the average square of the electron phonon scattering matrix on the Fermi surface [27]. In the case of strong coupling, the renormalized electron-phonon coupling is expressed as $^* \lambda_{PS}^{Coh} = \frac{\lambda_{PS}^{Coh}}{\lambda_{PS}^{Coh} + 1}$ [31].

When the pairing strength is calculated by the spin-unrestricted GGA-PBE functional without using the AF Ising Hamiltonian, this approach is defined as ‘traditional combination of DFT functional’. On the other hand, we propose an ‘empirical combination of DFT functional’. i.e. the average electron-phonon coupling in multi-energy layers is computed by the spin-restricted GGA-PBE functional [21-23] and further corrected by the AF Ising Hamiltonian. To include the magnetic effect, this AF Ising Hamiltonian must be acquired by the spin-unrestricted GGA-PBE functional.

The pairing strength formulas of LiFeAs (111-type), NaFeAs (111-type) and FeSe (11-type) under pressure are given as $\lambda_{11}^{111} = ^* \lambda_{PS}^{Coh} f_{11}^{111}(E_{ex})$ where $f_{11}^{111}(E_{ex}) \sim \frac{[M_{Fe} M_{Fe} E_{co}]_{P>0}}{[M_{Fe} M_{Fe} E_{co}]_{P=0}}$. The ratio $f_{11}^{111}(E_{ex})$ monitors the pressure dependence of the AF energy at each external pressure P where E_{co} is the exchange-correlation coupling.

We use $f_{11}^{111}(E_{ex})$ to correct the antiferromagnetism under pressure instead of recalculating the R_{SDW}^2 . We will compare the T_c values, which are acquired by the ‘empirical combination of DFT functional’ and ‘traditional combination of DFT functional’, respectively. The pairing strength is substituted into the McMillian T_c formula [27], which includes the enhanced electron-phonon scattering matrix elements:

$$T_c = \frac{T_{Debye}}{1.45} \exp \left(\frac{-1.04(1 + \lambda_{11}^{111})}{\lambda_{11}^{111} - \mu^* (1 + 0.62\lambda_{11}^{111})} \right)$$

3. Results

The atomic spring constants between the FeFe bond k_{FeFe} and FeSe bond k_{FeSe} in the iron-based superconductors are compared. Our DFT calculation shows that $k_{FeSe} / k_{FeFe} \sim 0.25$, while the k_{FeAs} is almost 2 times stronger than k_{FeSe} . As the atomic spring constants of the tetrahedral bonds are comparable to the FeFe bond, appearing the orthogonal phonon is feasible. Our two-channel model demonstrates that the induced xy potential is good enough be emerged at ‘GGA-PBE’ level. We calculated that the electron-phonon scattering matrix of FeSe under the induced xy -potential is amplified by $R_{ph}=2.8$. While the accuracy of our two-channel model is comparable to the $R_{ph}=2.2$ obtained from the calibrated GGA+A functional [18], we determine R_{ph} of NaFeAs and LiFeAs to be 1.97 and 1.8, respectively. The pressure dependence on R_{ph} is less than ~5% due to $c \gg a$.

A critical parameter in any ab-initio approach is the value of the renormalized Coulomb pseudopotential. Figure 1 estimates the error of the theoretical T_c by tuning μ^* . Despite the calculation of μ^* as a function of Debye temperature and Fermi level [31] may not be very accurate in such a strongly correlated electron system [32], it has been argued that for the most Fe-based superconductors μ^* should be 0.15-0.2 [33]. The error of our T_c calculation due to the uncertainty of μ^* is within ~15%. In this letter we choose the value ($\mu^*=0.15$) of the Coulomb pseudopotential to calculate the T_c of LiFeAs, NaFeAs and FeSe to make a fair comparison.

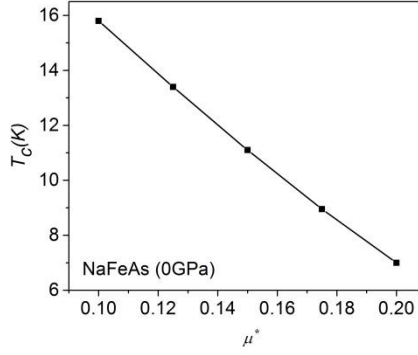


Figure 1. The theoretical T_c of NaFeAs varies slightly with the Coulomb pseudopotential. Our calculated μ^* -value of the uncompressed NaFeAs is 0.13.

Figure 2a shows that our approach can generate the theoretical T_c values in an appropriate range. The ARPES data confirms that LiFeAs and FeSe require the use of the R_g factor, while the NaFeAs does not [29, 30, 34]. The theoretical T_c of NaFeAs at 0GPa and 2GPa are 11K and 12.5K, respectively [35]. The antiferromagnetically enhanced electron-phonon interaction on the Fermi surface and the AF exchange Hamiltonian compete in the compressed NaFeAs as illustrated in Figure 2b. We observe that the antiferromagnetism is slightly weaker at finite pressure, but the antiferromagnetically assisted electron-phonon coupling on the Fermi layer is increased almost linearly at low pressure. We show the steps to estimate the T_c of NaFeAs at 0GPa as an example. After activating the spin-unrestricted mode, the R_{SDW}^2 is 1.625. The antiferromagnetically assisted electron-phonon coupling on the Fermi surface is $\lambda_{PS}^{Coh} = \lambda_{E_F} R_{SDW}^2 R_{ph}^2 R_g^2 = (0.13)(1.625)(1.97^2)(1^2) = 0.819$ and $\mu^* = 0.15$.

According to the McMillian T_c Formula, the T_c becomes

$$T_c = \frac{T_{Debye}}{1.45} \exp\left(\frac{-1.04(1 + \lambda_{11}^{111})}{\lambda_{11}^{111} - \mu^*(1 + 0.62\lambda_{11}^{111})}\right) = \frac{385}{1.45} \exp(-3.19) = 10.9K$$

We compare our theoretical T_c by substituting the raw data of other groups [15, 18], their calculated $\lambda_{E_F}^{AF}$ is 0.39 [15] and the induced xy potential by the out-of-plane phonon reinforces the electron-phonon coupling matrix by 2.2 [18].

$$\lambda_{PS}^{Coh} = \lambda_{E_F}^{AF} R_{ph}^2 R_g^2 = (0.39)(2.2^2)(1^2) = 1.88$$

After renormalization, these two couplings are softened to

$$\lambda_{11}^{111} = \lambda_{PS}^{Coh} = 1.88 / (1.88 + 1) = 0.652$$

And the renormalized Coulomb pseudopotential $\mu_{re}^* = \frac{\mu^*}{1 + \lambda_{PS}^{Coh}} = 0.15 / (1.88 + 1) = 0.052$.

The theoretical T_c becomes

$$T_c = \frac{T_{Debye}}{1.45} \exp\left(\frac{-1.04(1 + \lambda_{11}^{111})}{\lambda_{11}^{111} - \mu_{re}^*(1 + 0.62\lambda_{11}^{111})}\right) = \frac{385}{1.45} \exp(-2.97) = 13.6K$$

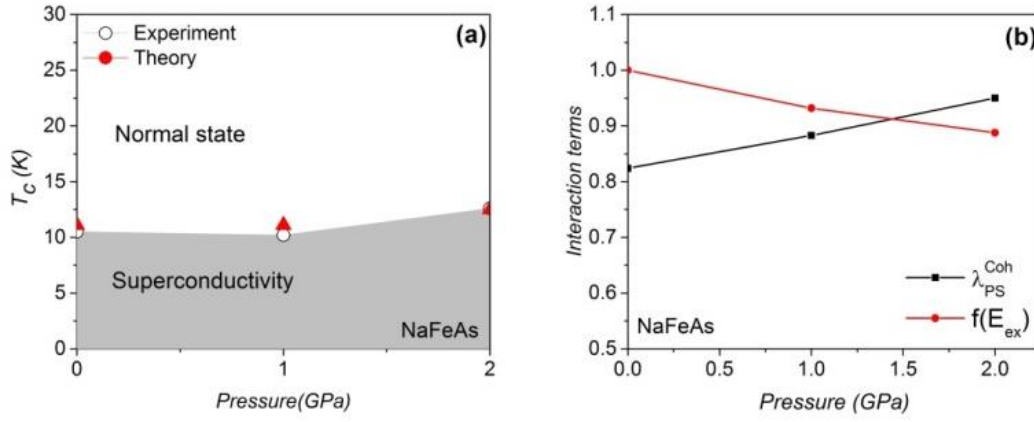


Figure 2. a The theoretical and experimental [35] T_c values of NaFeAs. b The antiferromagnetically assisted electron-phonon coupling on the Fermi surface and the AF energy as a function of pressure.

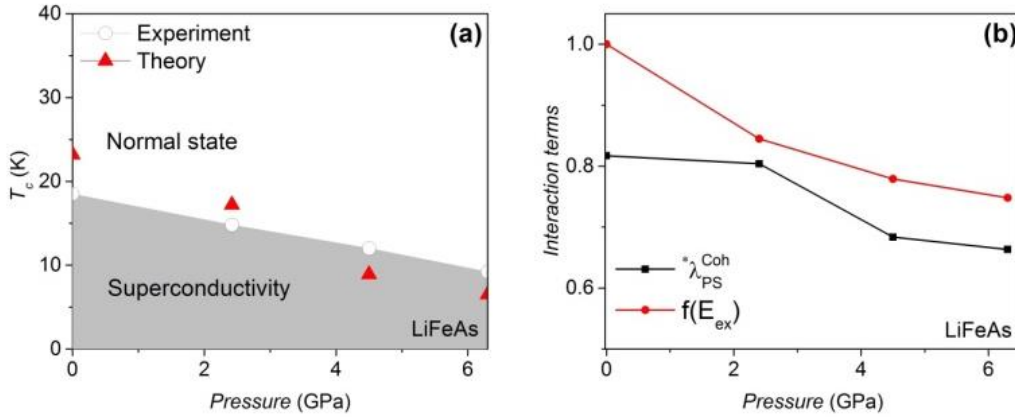


Figure 3. a The theoretical and experimental [36] T_c values of LiFeAs are consistent. b The antiferromagnetically assisted electron-phonon coupling and the AF exchange Hamilton under pressure. The R_{SDW}^2 equals to 1.75.

Our calculated value of the electron-phonon coupling on the Fermi surface of the uncompressed LiFeAs is ~ 0.1 [37] but the magnetic amplification factors increase the pairing strength to 0.82, remarkably. The Debye temperature T_{Debye} of LiFeAs remains at ~ 385 K below 8GPa [38], as shown in Table 1. A reduction of the theoretical T_c is also observed in the compressed LiFeAs and the weakening effect of λ_{PS}^{Coh} and $f_{11}^{111}(E_{ex})$ under pressure are identified, as shown in Figure 3b. In compressed FeSe [39], however, a gain in $f_{11}^{111}(E_{ex})$ is observed that triggers the increase of T_c under pressure (Figure 4). It should be noted that our approach is a mean field approach and we treat the spin fluctuations as being proportional to the mean field Hamiltonian. The vanishing of the macroscopic AF order observed in real samples is due to the strong fluctuation effects in these layered compounds. The magnetism considered here in the non-magnetic regimes of the phase diagrams is of a fluctuating microscopic nature. The optimized pairing strength of LiFeAs and FeSe is achieved at a pressure of 0GPa and 0.7GPa, respectively. The differences between $DOS(E_F - E_{Debye})$ and $DOS(E_F)$ in LiFeAs and FeSe are less than 4%. The R_g factor in LiFeAs is reduced with pressure, but the R_g factor of FeSe is optimized at medium pressure (see Table 1-2).

Table 1. The DFT parameter of LiFeAs. The R_g factor is compiled by the ‘empirical combination of DFT functional’.

P/GPa	a (Å)	c (Å)	FeAs length (Å)	R_g	T_{Debye} (K)
0	3.769	6.306	2.44	2.66	385.00
2.4	3.745	6.134	2.42	2.38	385.25
4.5	3.723	5.985	2.35	1.67	385.5
6.3	3.702	5.918	2.33	1.56	385.75

Table 2. The DFT parameter of FeSe. The R_g factor is simulated by the ‘empirical combination of DFT functional’.

P/GPa	a (Å)	c (Å)	FeSe length(Å)	R_g	T_{Debye} (K)
0	3.767	5.485	2.390	3.04	240
0.7	3.746	5.269	2.388	2.05	256
2.0	3.715	5.171	2.384	4.92	274
3.1	3.698	5.114	2.382	2.50	290

Table 3. The DFT parameter of NaFeAs. The R_g factor is computed by the ‘empirical combination of DFT functional’.

P/GPa	a (Å)	c (Å)	FeAs length(Å)	R_g	$T_{\text{Debye}}(\text{K})$
0	3.929	6.890	2.400	1.00	385.0
1	3.914	6.833	2.388	1.00	385.5
2.0	3.900	6.777	2.376	1.00	386.0

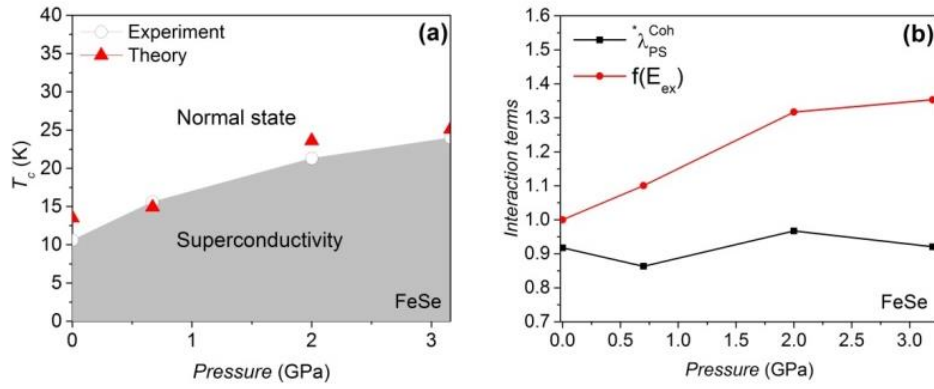


Figure 4. a Both theoretical and experimental [39] T_c values increase with pressure. b The pressure dependence of the antiferromagnetically assisted electron-phonon coupling and the AF interaction. The R_{SDW}^2 at 0GPa is 1.59.

4. Discussion

The pure FeAs layer in the 111-type, 1111-type and 122-type Fe-based superconductors is believed to trigger superconductivity [40]. The investigation of the pure FeAs layer without the Li and Na atoms in the simulation can show the bare pairing strength. The T_c vs. pressure of the NaFeAs is not as sensitive as for the other materials. The reason for this is that the increase of λ_{PS}^{*Coh} and the decrease of $f_{11}^{111}(E_{ex})$ almost cancel out the variation in the pairing strength.

The unusually high T_c in the LiFeAs and FeSe at 0GPa is mainly due to the R_{ph} , R_{SDW} and R_g factors. Our approach confirms that the reduction of T_c in compressed LiFeAs is mainly due to the decreases in λ_{PS}^{*Coh} and AF energy as a function of pressure. Conversely, the magnetic moment of Fe in FeSe increases under compression, resulting in an increase in AF energy under pressure. As a result, the increase of T_c in compressed FeSe is observed. The R_g factor is minimized at high pressure since the kinematics of electrons below the Fermi level is more restricted under pressure. Our simulation shows that the variation of the induced xy potential is less than $\sim 3\%$ for the electrons at ~ 100 meV below the Fermi level and therefore the use of the R_g factor in LiFeAs and FeSe is justified.

We correct the pairing strength at high pressures with help of the AF Ising Hamiltonian. In the following we compare the T_c when the R_{SDW} , R_g and R_{ph} are calculated by the spin-unrestricted GGA-PBE functional at high pressures or simply called the ‘traditional combination of DFT functional’. Despite the ‘traditional combination of DFT functional’ provides an accurate theoretical T_c at ambient pressure, the error of T_c is significant at high pressures. We demonstrate this for the case of FeSe in Table 4. In this approach we do not use the AF Ising Hamiltonian at finite pressure because magnetism is already considered. Since 2008, the R_g factor was missing in the calculation of the electron-phonon coupling constant. However, Table 5 confirms that the consideration of the electron-phonon coupling on the Fermi surface is not sufficient to argue whether iron-based superconductivity is mediated by phonons. If the R_g factor really participates in iron-based superconductivity, the abnormal distribution of electrons below the Fermi level should be given a larger range when the T_c of the iron-based superconductor is higher. This argument is supported by the ARPES data of the 100K 2D FeSe/SrTiO₃ [29]. For these ~ 30 K iron-based superconductors, the electrons located at 0.03eV-0.06eV below the Fermi level are affected by superconductivity [28, 30]. However, the electrons in the 100K 2D FeSe/SrTiO₃, which are located in a much wider range of 0.1eV-0.3eV below the Fermi level, participate superconductivity [29]. The theoretical T_c of the 2D FeSe/SrTiO₃ reaches 91K only if the R_g factor is considered [45].

Table 4. The theoretical T_c of FeSe at different pressures. Theoretical T_c (A) is obtained from the traditional combination of DFT functional. Theoretical T_c (B) is estimated from the empirical combination of DFT functional.

FeSe	Experimental T_c	Theoretical T_c (A)	Theoretical T_c (B)
0GPa	11K	13K	12K
0.7GPa	16K	4K	15K
2GPa	20K	3K	22K

Table 5. Effect of R_g factor on theoretical T_c values. The ‘empirical combination of DFT functional’ is used.

FeSe	Experimental T_c	Theoretical T_c (Without R_g factor)	Theoretical T_c (With R_g factor)
0GPa	11K	3K	12K
0.7GPa	16K	6K	15K
2GPa	20K	8K	22K
LiFeAs	Experimental T_c	Theoretical T_c (Without R_g factor)	Theoretical T_c (With R_g factor)
0GPa	19K	2K	23K
2.4GPa	15K	7K	17K
4.5GPa	13K	8K	9K
6.3GPa	10K	4K	7K

The T_c acquired by the ‘traditional combination of DFT functional’ fails at high pressures mainly because R_g is excessively suppressed. To monitor electron-phonon coupling under pressure, the use of the ‘empirical combination of DFT functional’ is a better choice. Although the accuracy of GGA-PBE functional may not be perfect, we

empirically correct the numerical output value λ_{11}^{111} directly via the AF Ising Hamiltonian and the two-channel model. On one hand, the two-channel model corrects the effect of the out-of-plane phonon at a low computational cost. On the other hand, the introduction of the induced xy potential in the electron-phonon calculation indirectly corrects the effect of the band diagram. The λ_{11}^{111} is controlled by the band diagram, which contains the information about the effective mass. The numerator and denominator in R_g are obtained from the same band diagram, so that the error due to the effective mass in these three non-heavy fermion superconductors can almost be cancelled.

It is still an open question which DFT functional is the best for iron-based superconductors. From an empirical point of view, the GW or screened hybrid functional is likely suitable for the unconventional bismuthate and the transition-metal superconductors [43]. The modelling of the Hubbard potential in the GGA+U approach provides a good agreement with the experimental results of BaFe_2As_2 and LaFeAsO [41]. Since the electron-electron interaction in the iron-based superconductors is complicated, the use of the highly correlated DFT functional should be reasonable. However, the T_c calculated with the screened hybrid functional HSE06 convinces us to use a different approach. We calculate the T_c of these three materials by the HSE06 functional, which is a class of approximations to the exchange–correlation energy functional in density functional theory, which includes a part of the exact exchange item from the Hartree–Fock theory with the rest of the exchange–correlation energy from other sources [43]. However, the exchange–correlation energy considered by the screened hybrid functional HSE06 does not suit the NaFeAs , LiFeAs and FeSe materials whose calculated T_c values become less than 0.1K. The more advanced approaches, such as GW or DMFT, can simulate most of the electronic properties of bulk FeSe closer to the experimental values but the major drawback is that the calculation of the electron–phonon coupling with these methods is based on a simplified deformation potential approximation, since electron–phonon coupling matrix elements are difficult to obtain [42].

The induced xy potential was rarely reported at GGA level. If the channels where the out-of-plane phonon cannot be hidden are considered separately, the GGA functional is already good enough to generate the induced xy -potential. If the lattice Fe moves orthogonally away from the xy plane in the iron-based superconductors, the electric charges in the xy plane are disturbed. Since the electronegativity of the tetrahedral atom (Se) is stronger, the electron will populate the FeSe bonds more [18]. For example, when the Fe moves along the $+z$ axis, the local electron density in the xy -plane changes. The induced charges have two possible paths, i.e. the electrons are shifted either above or below the xy plane to the FeSe bond [18]. However, the upward displacement of the Fe atom, which emits the electric field, confines the electrons more covalently in the upper tetrahedral region. The more covalently bonded FeSe interaction allows electrons to move out of the FeSe bond below the plane [18]. A charge fluctuation is created and generates the induced xy potential. Since the out-of-plane phonon is simulated by the two-channel model, the occurrence of the induced xy potential at GGA level means that the two-channel model has already taken the AF into account.

The McMillian formula takes into account the distribution of electrons in the form of a hyperbolic tangent (\tanh) function across the Fermi level [27]. At finite temperature, the Fermi-Dirac statistics fits the shape of the hyperbolic tangent function with the mean occupation number $f(E_F) = 0.5$. For example, elemental aluminum holds the superconducting transition temperature at 1.2K, where the offset $f(E_F - E_{Debye}) - f(E_F + E_{Debye})$ is 0.0056 at 3K. In addition, the offset $f(E_F - E_{Debye}) - f(E_F + E_{Debye})$ of elemental tin is 0.0028 at 3K. The McMillian formula provides the theoretical T_c of aluminum and tin correctly with the tiny offsets of 0.0056 and 0.0028, respectively. The relevant electrons in LiFeAs , NaFeAs and FeSe superconductors may be located in the energy range between $E_F - E_{Debye}$ and $E_F + E_{Debye}$, but their offsets $f(E_F - E_{Debye}) - f(E_F + E_{Debye})$ at the same temperature of 3K are as small as 0.0053, 0.0053 and 0.0034, respectively. If $f(E_F - E_{Debye}) - f(E_F + E_{Debye})$ in the iron-based superconductors are comparable to BCS superconductors, the numerical error due to the fitting of the relevant electrons indicated by the energy range we extracted from ARPES data as input in the McMillian formula and the Eliashberg function may not be obvious. If the R_g factor is introduced in a narrow energy range below the Fermi level, it fits even better to the \tanh function. Furthermore, the AF Ising model shows that the energy of the spin fluctuations is smaller than the Debye energy and hence the maximum integral in the McMillian derivation [27] cannot exceed the Debye temperature. Finally, none of the amplified electron-phonon couplings exceeds the limit of the straight-line fit for determining the empirical parameters [27]. Therefore, the McMillian formula becomes applicable in these three iron-based superconductors.

After we consider all electrons taking part in iron-based superconductivity between E_F and $E_F - E_D$, the T_c calculations of the above samples becomes accurate. We thus suggest that, given the relatively high transition temperatures of Fe-based superconductors at which a considerable amount of high energy phonons are excited, it is absolutely required to consider the entire energy range of electrons that can scatter up to the Fermi energy through these phonons, in contrast to the traditional low- T_c approaches, where the electronic density of states at the Fermi level can be used as an approximation. Despite our algorithm can produce the theoretical T_c of these three samples at reasonable values, further theoretical work is required to search for an ultimate flawless T_c formula that can estimate the theoretical T_c of all iron-based superconductors precisely.

5. Conclusion

After revising the superconducting electron-concentration in the McMillan T_c formula, we could show that when the conduction electrons interact with local Fe moments in Fe-based superconductors, the coexistence of superconductivity with local fluctuating antiferromagnetism [18] together with the abnormal lattice vibration [18-20], which can lead to an enormous increase in the electron phonon coupling, as predicted by these earlier theoretical studies [18-20], is sufficient to explain the high T_c values in an ab-initio approach based on the McMillan T_c formula. Our ab-initio approach can generate theoretical T_c values of NaFeAs, LiFeAs and FeSe close to the experimental values also depending on the applied pressure.

Acknowledgements

We thank Prof. Steven G. Louie in UC Berkeley Physics for his valuable suggestions

References

- [1] J G. Bednorz, K. A. Müller, Possible high T_c superconductivity in the Ba-La-Cu-O system, *Z. Phys. B* 64, 189-193 (1986).
- [2] M. Buchanan, Mind the pseudogap, *Nature (London)* 409, 8-11 (2001).
- [3] Y. Kamihara, T. Watanabe, M. Hirano, H. Hosono, Iron-Based Layered Superconductor $\text{La}[\text{O}_{1-x}\text{F}_x]\text{FeAs}$ ($x = 0.05-0.12$) with $T_c = 26$ K, *J. Am. Chem. Soc.* 130, 3296-3297 (2008).
- [4] M. R. Norman, High-temperature superconductivity in the iron pnictides, *Physics* 1, 21 (2008).
- [5] G. R. Stewart, Heavy fermion systems, *Rev. Mod. Phys.* 56, 755-787 (1984).
- [6] For a review see e.g. M. Lang, J. Mueller, Organic superconductors, in "The Physics of Superconductors - Vol. 2", K.-H. Bennemann, J. B. Ketterson (Eds.), Springer-Verlag (2003).
- [7] R. M. Fernandes, A. V. Chubukov, J. Schmalian, What drives nematic order in iron-based superconductors? *Nat. Phys.* 10, 97-104 (2014).
- [8] G. Grüner, The dynamics of charge-density waves, *Rev. Mod. Phys.* 60, 1129 (1988).
- [9] A. V. Chubukov, P. J. Hirschfeld, Iron-based superconductors, seven years later, *Physics Today* 68, 46-52 (2015).
- [10] D. J. Scalapino, Superconductivity and Spin Fluctuations, *J. Low Temp. Phys.* 117, 179-188 (1999).
- [11] V. L. Ginzburg, D. A. Kirzhnits (Eds.), High-Temperature Superconductivity, New York: Consultance Bureau, (1982).
- [12] P. J. Hirschfeld, M. M. Korshunov, I. I. Mazin, Gap symmetry and structure of Fe-based superconductors, *Rep. Prog. Phys.* 74, 124508 (2011).
- [13] W. Little, Possibility of Synthesizing an Organic Superconductor, *Phys. Rev.* 134, A1416 (1964).
- [14] V. L. Ginzburg, On surface superconductivity, *Phys. Lett.* 13, 101-102 (1964).
- [15] H. Kontani, S. Onari, Orbital-Fluctuation-Mediated Superconductivity in Iron Pnictides: Analysis of the Five-Orbital Hubbard-Holstein Model, *Phys. Rev. Lett.* 104, 157001 (2010).

- [16] S. Onari, H. Kontani, M. Sato, Structure of neutron-scattering peaks in both s_{++} -wave and s_{\pm} -wave states of an iron pnictide superconductor, *Phys. Rev. B* 81, 060504(R) (2010).
- [17] T. Saito, S. Onari, H. Kontani, Orbital fluctuation theory in iron pnictides: Effects of As-Fe-As bond angle, isotope substitution, and Z^2 -orbital pocket on superconductivity, *Phys. Rev. B* 82, 144510 (2010).
- [18] S. Coh, M. L. Cohen, S. G. Louie, Antiferromagnetism enables electron-phonon coupling in iron-based superconductors, *Phys. Rev. B* 94, 104505 (2016).
- [19] B. Li, Z. W. Xing, G. Q. Huang, M. Liu, Magnetic-enhanced electron-phonon coupling and vacancy effect in “111”-type iron pnictides from first-principle calculations, *J. App. Phys.* 111, 033922 (2012).
- [20] S. Deng, J. Köhler, A. Simon, Electronic structure and lattice dynamics of NaFeAs, *Phys. Rev. B* 80, 214508 (2009).
- [21] P. Blaha, K. Schwarz, G. K. H. Madsen, D. Kvasnicka and J. Luitz, WIEN2k, An Augmented Plane Wave + Local Orbitals Program for Calculating Crystal Properties (Karlheinz Schwarz, Techn. Universität Wien, Austria) (2001).
- [22] J. P. Perdew, J. A. Chevary, S. H. Vosko, K. A. Jackson, M. R. Pederson, D. J. Singh, C. Fiolhais, Atoms, molecules, solids, and surfaces: Applications of the generalized gradient approximation for exchange and correlation, *Phys. Rev. B* 46, 6671 (1992).
- [23] A. D. Becke, Density-functional exchange-energy approximation with correct asymptotic behavior, *Phys. Rev. A* 38, 3098 (1988).
- [24] M. Zhang, L.-M. He, L.-X. Zhao, X.-J. Feng, W. Cao, Y.-H. Luo, A density functional theory study of the Au₇Hn (n = 1-10) clusters, *J. Mol. Struct.: Theochem.* 911, 65-69 (2009).
- [25] Z. Hu, W. Xu, C. Chen, Y. Wen, L. Liu, First-Principles Calculations of the Structure Stability and Mechanical Properties of LiFeAs and NaFeAs under Pressure, *Adv. Mat. Sci. & Eng.*, 3219685 (2018).
- [26] M. Bendele, C. Marini, B. Joseph, L. Simonelli, P. Dore, S. Pascarelli, M. Chikovani, E. Pomjakushina, K. Conder, N. L. Saini, P. Postorino, Dispersive x-ray absorption studies at the Fe K-edge on the iron chalcogenide superconductor FeSe under pressure, *J. Phys.: Cond. Mat.* 25, 425704 (2013).
- [27] W. L. McMillian, Transition Temperature of Strong-Coupled Superconductors, *Phys. Rev.* 167, 331 (1968).
- [28] X.-W. Jia *et al.*, Common Features in Electronic Structure of the Oxypnictide Superconductor from Photoemission Spectroscopy, *Chin. Phys. Lett.* 25, 3765-3768 (2008).
- [29] C. Zhang *et al.*, Ubiquitous strong electron-phonon coupling at the interface of FeSe/SrTiO₃, *Nat. Commun.* 8, 14468 (2017).
- [30] U. Stockert, M. Abdel-Hafiez, D. V. Evtushinsky, V. B. Zabolotnyy, A. U. B. Wolter, S. Wurmehl, I. Morozov, R. Klingeler, S. V. Borisenko, B. Büchner, Specific heat and angle-resolved photoemission spectroscopy study of the superconducting gaps in LiFeAs, *Phys. Rev. B* 83, 224512 (2011).
- [31] K.-C. Weng, C. D. Hu, The p-wave superconductivity in the presence of Rashba interaction in 2DEG, *Sci. Rep.* 6, 29919 (2016).
- [32] E. J. König, P. Coleman, The Coulomb problem in iron based superconductors, arXiv:1802.10580 (2018).
- [33] [P. J. Hirschfeld *et al.*, Gap symmetry and structure of Fe-based Superconductors, *Rep. Prog. Phys.* 74 124508 (2011)
- [34] M. Yi, D. H. Lu, R. G. Moore, K. Kihou, C.-H. Lee, A. Iyo, H. Eisaki, T. Yoshida, A. Fujimori, Z.-X. Shen, Electronic reconstruction through the structural and magnetic transitions in detwinned NaFeAs, *New J. Phys.* 14, 073019 (2012).
- [35] A. F. Wang, Z. J. Xiang, J. J. Ying, Y. J. Yan, P. Cheng, G. J. Ye, X. G. Luo, X. H. Chen, Pressure effects on the superconducting properties of single-crystalline Co doped NaFeAs, *New J. Phys.* 14, 113043 (2012).
- [36] S. J. Zhang, X. C. Wang, R. Sammynaiken, J. S. Tse, L. X. Yang, Z. Li, Q. Q. Liu, S. Desgreniers, Y. Yao, H. Z. Liu, C. Q. Jin, Effect of pressure on the iron arsenide superconductor Li_xFeAs (x=0.8, 1.0, 1.1), *Phys. Rev. B* 80, 014506 (2009)
- [37] R. A. Jishi, D. Scalapino, Contribution of the electron-phonon coupling to the pairing interaction in LiFeAs, *Phys. Rev. B* 88, 184505 (2013).

- [38] L. Liu, G. Xu, A. Wang, X. Wu, R. Wang, First-principles investigations on structure stability, elastic properties, anisotropy and Debye temperature of tetragonal LiFeAs and NaFeAs under pressure, *J. Phys. & Chem. Solids* 104, 243–251 (2017).
- [39] S. Masaki, H. Kotegawa, Y. Hara, H. Tou, K. Murata, Y. Mizuguchi, Y. Takano, Precise Pressure Dependence of the Superconducting Transition Temperature of FeSe: Resistivity and ^{77}Se -NMR Study, *J. Phys. Soc. Jpn.* 78, 063704 (2009).
- [40] J. P. Paglione, R. L. Greene, High-temperature superconductivity in iron-based materials, *Nat. Phys.* 6, 645-658 (2010).
- [41] J. K. Jang and J. Y. Rhee, Magnetic States of Iron-based Superconducting Compounds: A Comparative Study with Fe_3Al Alloy, *J. Kor. Phys. Soc.* 66, 646-650 (2015).
- [42] S. Coh, M. L. Cohen and S. G. Louie, Large electron–phonon interactions from FeSe phonons in a monolayer, *New J. Phys.* 17, 073027 (2015).
- [43] Z. P. Yin, A. Kutepov, and G. Kotliar, Correlation-Enhanced Electron-Phonon Coupling: Applications of GW and Screened Hybrid Functional to Bismuthates, Chloronitrides, and Other High-Tc Superconductors, *Phys. Rev. X* 3, 021011 (2013).
- [44] J. M. Kosterlitz, The critical properties of the two-dimensional xy model, *J. Phys. C* 7, 1046 (1974).
- [45] C. H. Wong, R. Lortz, The interactions between antiferromagnetism, tetrahedral sites and electron-phonon coupling in $\text{FeSe}_{1-x}\text{Te}_x$ and $\text{FeSe}/\text{SrTiO}_3$, arXiv:1905.13426